Photon Netw Commun (2016) 31:1–10
DOI 10.1007/s11107-015-0523-1

Energy efficiency in optical CDMA networks with forward error correction

Fábio Renand Durand[1] · Taufik Abrão[2]

Received: 18 December 2014 / Accepted: 13 June 2015 / Published online: 24 June 2015

Abstract In this work, we investigate the energy efficiency in optical code division multiplexing access (OCDMA) networks with forward error correction (FEC). We have modeled the energy efficiency considering the capacity of information transmitted and the network power consumption. The proposed network power consumption model considers the optical transmitter, receiver, optical amplifiers, FEC and network infrastructure as encoders, decoders, star coupler and network control in the overall optical power network consumption balance. Furthermore, an expression relating the signal-to-noise-plus-interference ratio gain for forward error correction with low-density parity-check code scheme considering the power consumption and bandwidth occupancy has been derived. Numerical results for OCDMA networks with aggregated FEC procedure have revealed the viability of the FEC deployment aiming to increase the overall energy efficiency of OCDMA networks.

Keywords Optical code division multiplexing access · Energy efficiency · Power consumption · Forward error correction

✉ Taufik Abrão
taufik@uel.br

Fábio Renand Durand
fabiodurand@utfpr.edu.br

1 Technological Federal University of Paraná, UTFPR, CP 6101, Cornélio Procópio, PR, Brazil

2 Department of Electrical Engineering, State University of Londrina, UEL-PR, Londrina, Brazil

1 Introduction

The increase in the diversity and volume of traffic transmitted in all the scales of networks results in a multitude of efforts and initiatives to improve the technology of transmission, switching, control and management of optical networks [1, 2]. Furthermore, the increase in the spectral efficiency (SE) and energy efficiency (EE) have been largely investigated for advancing toward more efficient, flexible and scalable solutions [3–5]. In this context, the increase in the heterogeneous set of requirements caused by massive intensification of content delivery networks and data centers is spurring rapid growth in metro-only Internet traffic [1]. Moreover, the advance of the technologies as optical code division multiple access (OCDMA), orthogonal frequency division multiplexing (OFDM) and wavelength division multiplexing (WDM) is strategic to support the traffic requirements [2,6].

In the last years, OCDMA-based networks have attracted a lot of interests due to its various advantages including asynchronous operation, high network flexibility, protocol transparency, simplified network control and potentially enhanced security [7]. Despite of the physical impairments restrictions of the OCDMA transmission schemes for long distances [8–10], this technology is very attractive to meet a broad range of services with different and variable demands of bit rate requirement, connection duration, frequency of use and setup time for metropolitan area networks coverage. In OCDMA networks, each different code defines a user and different code users can share a common channel. In a common channel, the interference that may arise between different code users is known as multiple access interference (MAI) and can limit the number of code users utilizing the channel simultaneously [7]. Furthermore, the establishment of conditions for transmissions with a higher optical signal-to-noise-plus-interference ratio (SNIR) allows us to reduce the number of retransmissions by higher layers, thus increasing network throughput [11].

An effective approach to compensate the SNIR degradation in OCDMA systems with low hardware investment cost and high error-correction performance can be achieved with the FEC coding technique [12,13]. This technique is based on adding the redundant information previously to the modulation and transmission processes. The FEC techniques can be classified into three generations [14]. The first generation of FEC was based on the hard-decision decoding technique that uses block codes, in which a typical example is the Reed–Solomon (RS) codes, such as RS (255, 239). The second generation of FEC is mainly focused on the use of concatenated codes as RS and Bose, Chaudhuri and Hocquenghem (BCH) codes, e.g., RS (255, 239)/BCH (1023, 963). The third generation of FEC is based on more powerful soft-decision codes such as low-density parity-check code (LDPC) and block turbo codes, e.g., LDPC (4161, 3431).

OCDMA systems can be divided into non-coherent (unipolar) and coherent (bipolar) systems. The non-coherent systems are based only on intensity modulation of optical power, and coherent systems are based on modulation of amplitude and phase [7]. The coherent code is true-orthogonal, while non-coherent code is pseudo-orthogonal. The non-coherent codes can be classified into one-dimensional (1D) and two-dimensional (2D) codes [2]. In 1D codes, the bits are subdivided temporally into many short chips with a designated chip pattern representing a user's code. On the other hand, in 2D codes the bits are subdivided into individual time chips, and each chip is assigned to an independent wavelength from a discrete set of wavelengths [2]. The 2D codes have better performance than 1D codes and can significantly enhance the number of active and potential users [7]. In this work, 2D codes have been deployed considering their performance and the technological maturity [15].

The first and second FEC generations are not efficient to correct errors in non-coherent 2D OCDMA [16,17]. The non-coherent OCDMA systems are not symmetrical due to the asymmetry of MAI and noise [17]. Besides, when an optimal threshold is chosen, it is not clear whether 1's or 0's will suffer from the highest error probability. It usually changes, depending on the number of active users and noise distribution [17]. Furthermore, in order to enhance the performance of the error-correction coding block, it is necessary to take into account the channel unbalance and the specific MAI distribution at the decoder side. Moreover, there is a significant improvement when FEC based on soft-decision codes are adopted in OCDMA networks [16–18]. The efficacy of FEC schemes for energy-efficient transmission mode in OCDMA networks has not been investigated properly in terms of energy consumption estimation for performing encoding and decoding operations.

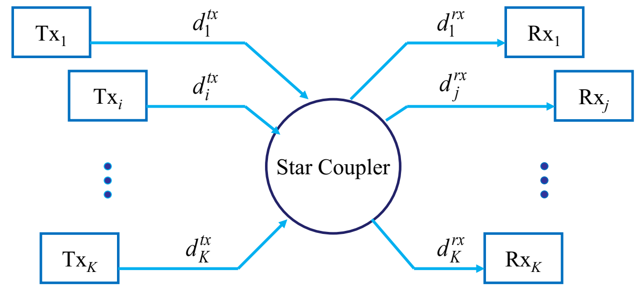

Fig. 1 OCDMA network architecture

In this context, the objective of this work is the investigation of the energy efficiency in OCDMA networks with FEC based on soft-decision LDPC codes. In this work, the energy efficiency of OCDMA networks will be modeled considering the network capacity and overall power consumption of OCDMA networks based on 2D codes (time/wavelength). Our network power consumption model considers the optical layer composed by transmitter, receiver, optical amplifiers, FEC and network infrastructure as encoders, decoders, star coupler and network control. The objective is to establish the trade-off between FEC utilization and optical layer energy efficiency in OCDMA networks.

2 Network architecture

The OCDMA network considered in this work is formed by $K \times K$ nodes interconnected by passive star coupler, in a broadcast-and-select pattern as shown in Fig. 1. The transmitting and receiving nodes create virtual path based on the code, while the total link length is determined by $d_{ij} = d_i^{tx} + d_j^{rx}$, where d_i^{tx} is the link length from the transmitting node to the star coupler and d_j^{rx} is the link length from the receiving node to the star coupler. The received power at a jth node is given by $P_{rj} = a_{\text{star}} p_i \exp\left(-\alpha_f d_{ij}\right)$, where p_i is the transmitted power by ith transmitter node, α_{f} is the fiber attenuation (km^{-1}) and a_{star} is the star coupler attenuation (linear units). Considering decibel units, $a_{\text{star}} = 10 \log(K) - \left[10 \log_2(K) \log_{10} \delta\right]$, where δ is the excess loss ratio. For viability characteristics, we consider network equipment, such as code-processing devices, including encoders and decoders at the transmitter and receiver and star coupler; those devices could be made using robust, lightweight and low-cost technology platforms with commercial off-the-shelf technologies [15].

In the 2D wavelength-hopping/time-spreading code sequence OCDMA networks, the code is transmitted and its destination node in the network is determined by a particular code sequence [15]. The 2D codes can be represented by $N_\lambda \times N_{\text{T}}$ matrices, where N_λ is the number of rows, which is equal to the number of available wavelengths, and

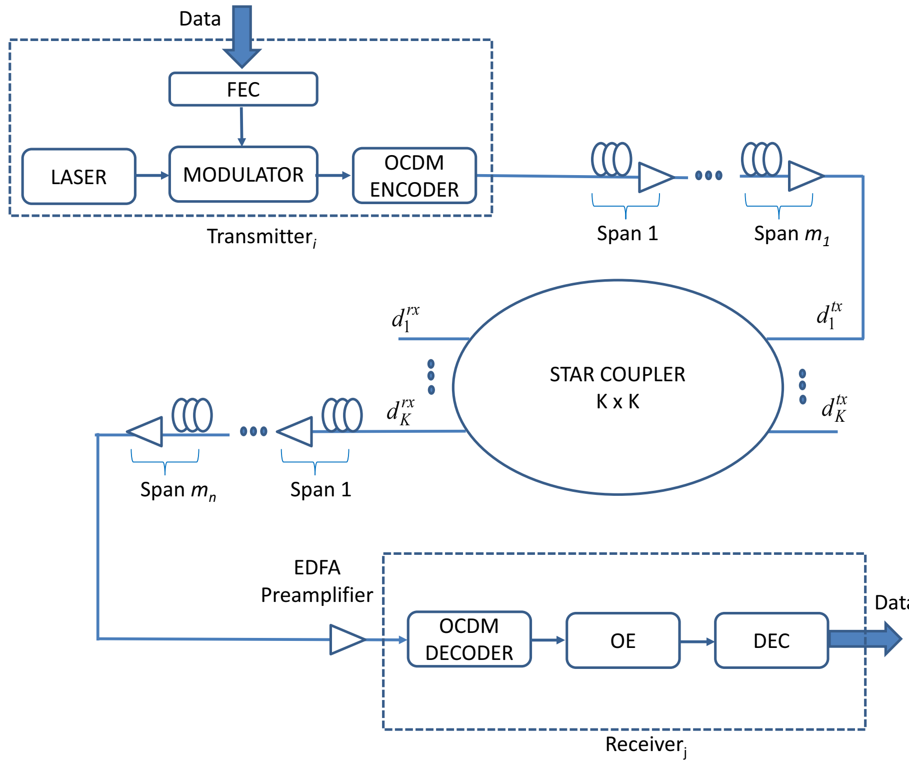

Fig. 2 Block diagram of OCDMA system

N_T is the number of columns, which is equal to the code length [7]. The code length is determined by the bit period T_B which is subdivided into small units called chips, each of duration $T_c = T_B/N_T$. In each code, there are w short pulses of different wavelength, where w is called the weight of the code. A code defined by $(N_\lambda \times N_{T,} w, I_a, I_c)$ is a collection of binary $N_\lambda \times N_T$ matrices each of code weight w; I_a and I_c are nonnegative integers and represent the constraints on the autocorrelation and cross-correlation [2], respectively.

2.1 Block diagram of transmission system

In this work, the block diagram illustrated in Fig. 2 represents the end-to-end virtual path. This block diagram depicts a generic set of components from transmitter, optical fiber spans with optical amplifiers, star coupler and receiver. Generally, the OCDMA networks use optical amplifiers only as preamplifier at the receiver side [11]; however, considering the extension reached with passive optical networks (PONs) [6], it is possible to consider more than one amplifier or span in our model.

In the OCDMA transmitter, the incoming data stream is encoded with FEC–LDPC-based codes. This encoded signal will modulate the laser output that can be implemented using multi-wavelength sources such as light-emitting diodes, amplified spontaneous emission noise from erbium-doped fiber amplifier (EDFA), gain switched Fabry–Pérot lasers and supercontinuum generation [15]. These sources avoid the need for rapid wavelength hop according to the wavelength-hopping pattern. Data modulation is done either before or after the encoding, depending on the transmitter design and network application. In our model, the modulated signal is encoded into a pseudorandom optical code by the OCDMA encoder that selects w pulses of N_λ wavelengths and arrange them within N_T chips of the bit interval as prescribed by the code sequence. Thus, the encoder essentially performs two processes: wavelength hopping and time spreading. The common technology applied in encoders/decoders with delay lines is array waveguide gratings (AWGs), thin-film filters (TFFs), simultaneously as fiber Bragg gratings (FBGs), holographic Bragg reflectors (HBRs) and chirped Moire gratings (CMGs) [2,11,15]. Then the encoded optical CDMA signal is attenuated by the fiber connecting the transmission node to the star coupler, and optical amplifiers are used in each span for compensating the fiber attenuation. The star coupler broadcasts the optical signal to all receiver nodes, so that at the receiving node we have the desired and interfering users signals. At the receiver, the OCDMA decoder recognizes the optical codes by performing a correlation process, where the autocorrelation for the target optical code produces high-level output, while the cross-correlation for undesired optical codes produces low level output. Finally, the FEC data can be recovered after threshold and decoding (DEC) operations are conducted to recover the original transmitted signal. The illustrated scheme can be easily adapted for case without FEC, considering the retraction of the FEC/DEC blocks in the Fig. 2.

3 Energy efficiency and power consumption model

Our power consumption model is based on the block diagram illustrated in Fig. 2. The objective is the establishment of the power consumption contribution of the main blocks involved in the overall communication process. Furthermore, the power consumption of the ith optical code path is given by

$$P_{\text{Optical}_i} = P_{\text{TX}_i} + P_{\text{RX}_j} + \sum P_{\text{EDFA}_{ij}} + P_{\text{Control}} \tag{1}$$

where P_{TX_i} is the power consumption of the transmitter, P_{RX_j} is the power consumption of the receiver, $P_{\text{EDFA}_i j}$ is the power consumption of the each EDFA in the optical route (in-line and at the receiver) and P_{Control} is the power consumption of the control scheme. The P_{TX_i} is calculated considering the following components:

$$P_{\text{TX}_i} = \frac{R_i}{\eta_{\text{EO}}}\left(E_{\text{FEC}} + E_{\text{MOD}}\right) + \frac{\eta_{\text{T}} R_i}{2} + P_{\text{CW}} \tag{2}$$

where R_i is the bit rate at ith node, $\eta_{\text{EO}} \in (0; 1]$ is the relative electro-optical power conversion efficiency, $\eta_{\text{T}} \in [0; 1]$ is the transponder efficiency, and P_{CW} is the laser continuous wave output power of the modulator. E_{FEC} is the FEC encoding energy consumption, and E_{MOD} is the modulator energy consumption, both in (J/bits).

Besides, the FEC encoding energy consumption is based on the LDPC encoding energy consumption (E_{LPCD}) [19], described by:

$$E_{\text{FEC}}\left(l, k\right) = \frac{\left[\left(l-k\right)\left(kc_g - 1\right) E_{\text{op}}^{G} + l E_{\text{op}}^{R}\right]}{k} \tag{3}$$

where l is the code length, k is the number of information bits per code block, c_g is the generator matrix average ratio of ones per column, E_{op}^{G} and E_{op}^{R} are the average energy per gate operation and register access, respectively. The other elements of (2) are given by (4) and (5) from [4].

$$E_{\text{MOD}} = \frac{8 V_{\text{cc}} V_{\text{pp}}}{R_{\text{T}} R_i} \tag{4}$$

$$P_{\text{CW}} = I_i \cdot 10^{L_{\text{mod}}/10} \tag{5}$$

where V_{cc} is the modulator driver supply voltage, V_{pp} is the modulator peak to peak swing voltage, R_{T} is the modulator and driver termination resistance, I_i is the input launch power for the ith node and L_{mod} is the optical excess loss of the modulator.

The P_{RX_j} is calculated considering the following elements:

$$P_{\text{RX}_j} = \frac{R_i}{\eta_{\text{EO}}}\left(E_{\text{OE}} + E_{\text{DEC}}\right) \tag{6}$$

where E_{DEC} is the energy consumption for decoding and E_{OE} is the optical/electrical converter energy consumption in [J/bits], given by [4]:

$$E_{\text{OE}} = \frac{16 \Re V_{\text{bias}} P_{\text{rec}}}{R_i} \tag{7}$$

where $\Re$ is the photodiode responsivity in (A/W), V_{bias} is the photodiode bias voltage and P_{rec} is the received power in [W]. In the case without FEC, E_{FEC} and E_{MOD} are considered zero.

The power consumption of the optical amplifier in the optical node and in-line configuration considering automatic gain control (AGC) is given by [4]

$$P_{\text{EDFA}_i} = \frac{P_{\text{in}}\left(G_{\text{AMP}}\left(\omega\right) - 1\right)}{\eta_E \eta_{\text{PCE}}} \tag{8}$$

where P_{in} is the optical power amplifier input, $\eta_{\text{PCE}} \in (0; 1]$ is the amplifier power conversion efficiency, $\eta_E \in (0; 1]$ is the power conversion efficiency of the amplifier control and management circuitry, including the temperature controllers and the pump laser. The efficiency parameters are related by $\eta_{\text{EPCE}} = \eta_E \times \eta_{\text{PCE}}$. The spectral gain ($G_{\text{amp}}$) is given by [20]

$$G_{\text{amp}}\left(\omega\right) = \frac{G_0\left(\omega\right)}{1 + P_{\text{out}} \big/ P_{\text{sat}}} \tag{9}$$

where $G_0\left(\omega\right)$ is the spectral non-saturated amplifier gain, P_{out} is the optical power amplifier output, and P_{sat} is the optical power amplifier saturation. Besides, G_{amp} depends on the optical power at amplifier input.

The power consumption for each node to perform the information processing, power control and SNIR estimation in the receiver is adapted from [21],

$$P_{\text{Control}_i} = P_{\text{CP}} + K\, P_{\text{CN}} \tag{10}$$

where K is the number of nodes, P_{CP} is the power consumption of the control plane which is divided for all nodes, and P_{CN} is the power consumption of the node unit for control information and processing.

4 Energy efficiency in OCDMA networks

The energy efficiency in the OCDMA networks can be formulated from the point of view of energy efficiency definition as the ratio of the sum of channel capacity of each optical code path and the sum of power consumption of all these optical code paths. From the Shannon information theory, the capacity of a channel can be described as the asymptote of the rates of transmission of information, which can be achieved with arbitrarily low error rate [22]. Therefore, the energy efficiency in [bits/J] of the optical network can be described as

$$\eta_E = \frac{\sum_{i=1}^{K} B_i \log_2 (1 + \gamma_i/\Gamma_i)}{\sum_{i=1}^{K} P_{\text{Optical}_i}} \tag{11}$$

where P_{Optical_i} is the power consumption of the ith node, defined by Eq. (1), Γ_i is the gap constant, which is utilized to separate coding gain from power allocation gain [23]. For uncoded modulation, the gap constant is given by [23]

$$\Gamma_i = \frac{\theta_i^2}{3} \tag{12}$$

where $\theta_i = Q^{-1}(P_e)$, P_e is the symbol error probability, and Q^{-1} is the inverse Q function. Finally, γ_i is the ith optical code SINR. Assuming single-rate case, the SINR for the ith node of a 2D code OCDMA system can be precisely written as [24],

$$\gamma_i = \frac{N_T^2 g_{ii} p_i G_{\text{amp}}}{\sigma_2 G_{\text{amp}} \sum_{j=1, j\neq i}^{K} g_{ij} p_j + 2N_{\text{eq}}} \tag{13}$$

where g_{ij} and G_{amp} are, respectively, the total loss and total amplifier gain in the path that connects ith-Tx node to jth-Rx node. For links without others EDFAs, G_{amp} represents the gain of the preamplifier. Parameter g_{ij} encompasses the fiber attenuation and power losses caused by encoders, decoders and star coupler, as discussed in previous section. σ^2 is the average variance of the Hamming aperiodic cross-correlation amplitude [8]. N_{eq} is the spontaneous amplified emission (ASE) noise power accumulation in chains of optical amplifiers, including the preamplifier at the receiver, according to the recursive model presented in [9]. The noise contribution of each amplifier (N_{ASE}) is given by,

$$N_{\text{ASE}} = n_{\text{SP}} h f \left(G_{\text{amp}} - 1\right) B_i \tag{14}$$

where n_{sp} is the spontaneous emission factor, typically around 2–5, h is Planck's constant, f is the carrier frequency, and B_i is the optical bandwidth. At the usual OCDMA receiver, the noise power includes thermal noise, shot noise and optical preamplifier noise. However, ASE in the optical preamplifier will be the main limiting factor (in addition to the MAI), compared to thermal and shot noise at the receiver [11].

It is worth noting that both transmission power and optical layer power consumptions are very important factors for energy-efficient optical communication; furthermore, the energy efficiency and the transmitted power of each node (I_i) will be affected by the minimum SNIR required by the FEC. In our work, the optimum transmitted power of each node is related to the SNIR optimization according to the distributed power control algorithm (DPCA) [11]. The efficient power control is needed to overcome the MAI and near–far problem, besides it enhances the performance and throughput of the network [25]. The classical DPCA synthesis consists of the development of a systematic procedure for the transmitted power (I_i) evolution in order to reach the optimum value I_i^*, based on the target SNIR γ_i^*, γ_i and I_i values [11,25]. The optimum solution for the power allocation problem satisfies the following associate iterative process [25],

$$I_i[n+1] = I_i[n] - \alpha \left(1 - \frac{\gamma_i^*}{\gamma[n]}\right) I_i[n] \tag{15}$$

where n is the number of iterations and α is the convergence factor or the numerical integration step that converges for $0 < \alpha < 1$. This equation represents the classical DPCA proposed by Foschini and Miljanic for CDMA wireless network, and it can be effectively adapted in each optical node for optical networks [11]. This DPCA could be implemented in each optical node because all necessary parameters (SNIR level given by γ_i^* and the transmitted power $I_i[n]$) are known in the node. Thus (15) depends on local parameters just allowing that the power control works in a distributed manner. Convergence issues and existence of the DPCA equilibrium have been extensively explored in the literature and will not be treated herein [11].

4.1 Transmitted power and energy efficiency improvement with FEC

The energy efficiency and the transmitted power of each node will be affected by the gain of the SNIR proportionated by the FEC deployment. Indeed, for OCDMA system with FEC, the energy efficiency can be described as:

$$\eta_E = \frac{\sum_{i=1}^{K} B_i^{\text{FEC}} \log_2 \left(1 + \gamma_i^{\text{FEC}}/\Gamma_i^{\text{FEC}}\right)}{\sum_{i=1}^{K} P_{\text{Optical}_i}^{\text{FEC}}} \tag{16}$$

where $B_i^{\text{FEC}} = (1 + h_{\text{FEC}}) B_i$, h_{FEC} is the FEC overhead and $P_{\text{Optical}_i}^{\text{FEC}} = P_{\text{Optical}_i}^{F} + \frac{R_i}{\eta_{\text{EO}}} (E_{\text{FEC}} + E_{\text{DEC}})$; also, $P_{\text{Optical}_i}^{F}$ is the power consumption of the ith optical code path with FEC, γ_i^{FEC} is the SNIR for FEC OCDMA scheme, and Γ_i^{FEC} is the FEC gap constant. Without loss of generality, if only one optical code path is considered, then (11) is equably with (16) for the same energy efficiency. In this context, the SNIR with FEC will be given by:

$$\gamma_i^{\text{FEC}} = \gamma_i \frac{\Gamma_i^{\text{FEC}}}{\Gamma_i} 2^{\Theta} \tag{17}$$

where Θ represents the ratio of the power consumption of OCDMA with and without FEC, which is described as:

$$\Theta = \frac{P_{\text{Optical}_i}^{\text{FEC}}}{(1 + h_{\text{FEC}}) P_{\text{Optical}_i}} \tag{18}$$

Fig. 3 Distance between Tx nodes to star coupler and distance between Rx nodes to star coupler for **a** 8, **b** 16 and **c** 32 nodes, respectively

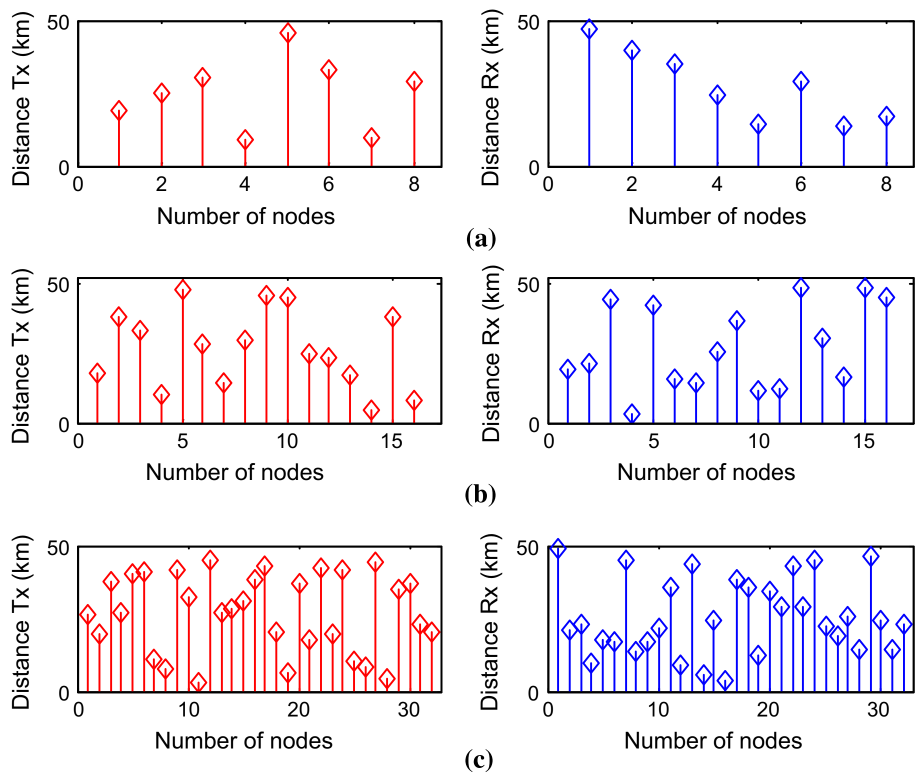

5 Numerical results

The scenarios considered in our study are characterized in Fig. 3 for OCDMA networks with (a) 8, (b) 16 and (c) 32 nodes. The nodes are uniformly distributed over a physical area with a radius in between 2 and 50 km; hence, the range of the total optical link length is [4; 100] km. This studied topology is general enough either to be applied in the standard patterns, such as 10GE-PON [2] or to support the increasing number of the nodes connected to each remote node [6]. Tables 1 and 2 illustrate the adopted values for the power consumption variables and the optical fiber link parameters, respectively. Typical parameters of devices, components and equipment were assumed for 2D codes $(4 \times 101, 4, 1, 0)$, with the transmission rate of 10 Gbps [4,5,15,18]. The AWG encoder/decoder has approximately uniform loss (6 dB)

Table 1 Power consumptions variables

Parameter	Adopted value
η_{EO}—Power conversion efficiency	1 %
η_T—Transponder efficiency	5 (W/Gbps)
E_{op}^G—Energy per gate operation	$0.69 p_t V^2$ (fJ)
E_{op}^R—Energy per register access	$3.43 p_t V^2$ (fJ)
c_g—Average ratio of ones per column	0.5
E_{DEC}—Energy consumption for decoding	8.6 (pJ/bit)
p_t—CMOS feature size	100 (nm)
V—CMOS supply voltage	0.8 (V)
V_{cc}—Modulator driver supply voltage	5.2 (V)
V_{pp}—Modulator peak swing voltage	8 (V)
R_T—Modulator termination resistance	50 (Ω)
L_{mod}—Optical excess loss	2.5 (dB)
$\Re$—Photodiode responsivity	0.9 (A/W)
V_{bias}—Photodiode bias voltage	3.3 (V)
η_{EPCE}—EDFA conversion efficiency	1 %
P_{CP}—Control plane consumption	300 (W)
P_{CN}—Node processor consumption	17 (W)

Table 2 Optical fiber link parameters

Parameter	Adopted value
α_f—Fiber loss coefficient	0.2 (dB/km)
L_s—Span length	65 (km)
h—Planck constant	6.63×10^{-34} (J/Hz)
f—Light frequency	193.1 (THz)
B_o—Optical bandwidth	30 (GHz)
n_{sp}—Spontaneous emission factor	2
δ—Excess loss ratio	0.2 (dB)
P_{sat}—EDFA power saturation	16 (dBm)
G_0—Spectral EDFA gain	$15 - 4 \times 10^{16} \left(\lambda - 1555 \times 10^{-9}\right)^2$
BER—Bit error rate	10^{-9}
BER_{FEC}—Bit error rate for FEC	10^{-3}

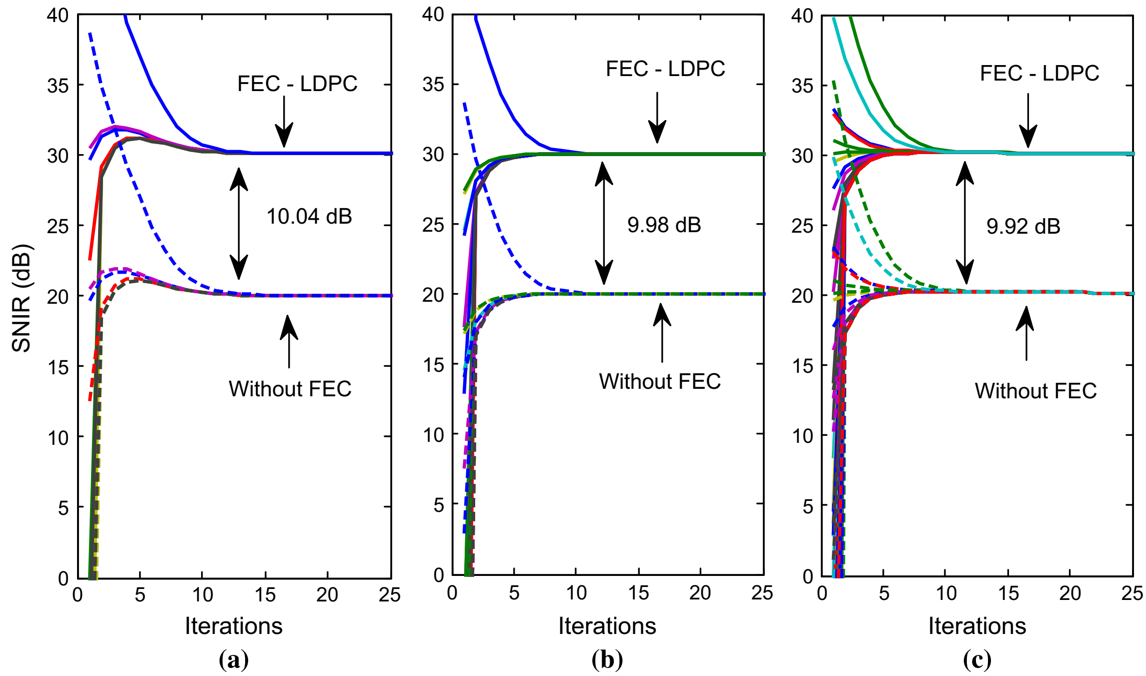

Fig. 4 SNIR evolution as a function of the number of iterations for **a** 8, **b** 16 and **c** 32 nodes with FEC and without FEC

independently of number of wavelengths (N_λ) [15]. The ASE noise is larger than all other kinds of noises at the receiver side, and all receiver nodes utilize an optical preamplifier that contributes with gain and noise power; this fact justifies the consideration of ASE noise in optical links in the networks with length less than 60 km. The LDPC code (905, 725, 0.8011) with overhead of 24.8 % and limit of SNIR of 14.6 dB was chosen. This FEC could correct a bit error rate (BER) of 10^{-3} to achieve the value of 10^{-9}. The factor of convergence (α) adopted is 0.5. This value allows combining a relative fast convergence velocity with acceptable quality of the solution after 40–50 iterations [25].

Figure 4 shows the SNIR evolution for the number of iterations of the classical DPCA in Eq. (15), considering (a) 8, (b) 16 and (c) 32 nodes for FEC–LDPC and without FEC schemes with DPCA. The energy efficiency is the same for the schemes with FEC and without FEC. The goal is to quantify the impact on the SNIR improvement with the FEC deployment, as well as the trade-off between SNIR gain, power consumption and the optical network size (number of node increasing).

Furthermore, it can be observed from Fig. 4 that the SNIR reaches the convergence after low number of iterations for both the FEC–LDPC and without FEC schemes. Indeed, the SNIR for FEC–LDPC is higher than the SNIR without FEC in approximately 10.04, 9.98, 9.92 dB for 8, 16 and 32 nodes, respectively. These gains in the SNIR for FEC–LDPC scheme are obtained through the FEC encoding/decoding process that results in the additional power consumption

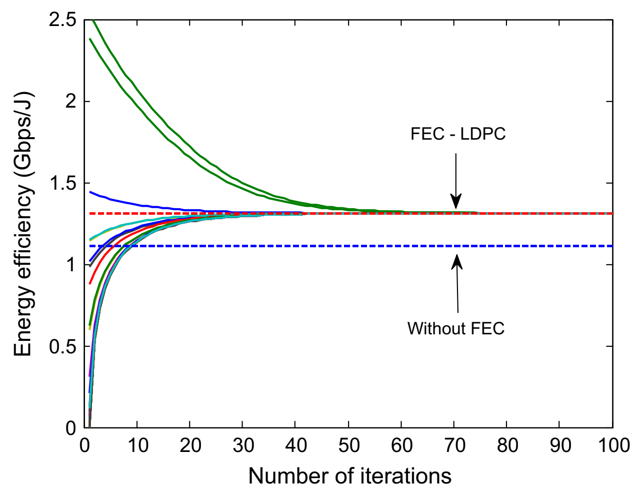

Fig. 5 Energy efficiency evolution as a function of the number of iterations for 32 nodes. The maximum energy efficiency allowed is represented by *horizontal lines* (*dash*) for the cases with FEC and without FEC

and increase in the required bandwidth. The SNIR gain for FEC–LDPC scheme could be obtained analytically with (17) resulting in approximately 10.09, 9.95 and 9.81 for 8, 16 and 32 nodes, respectively. Therefore, the SNIR gain for FEC–LDPC scheme could be forested analytically or numerically with DPCA with agreement in the results.

Figure 5 depicts the energy efficiency evolution as a function of the number of iterations of the classical DPCA, Eq. (15), considering 32 nodes for the FEC–LPCD. The max-

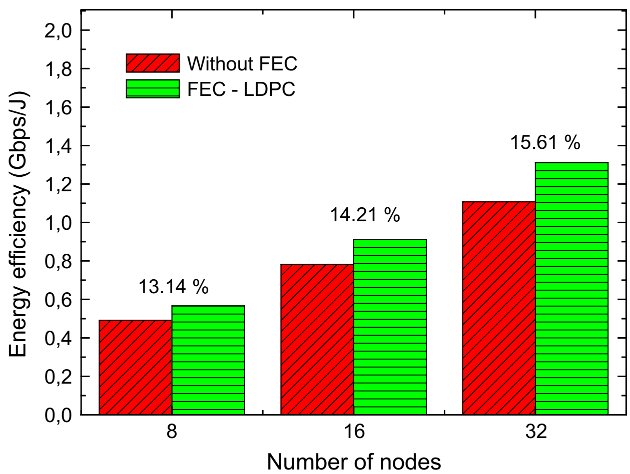

Fig. 6 Energy efficiency for OCDMA networks with different sizes for 8, 4 and 32 nodes, considering cases with FEC and without FEC

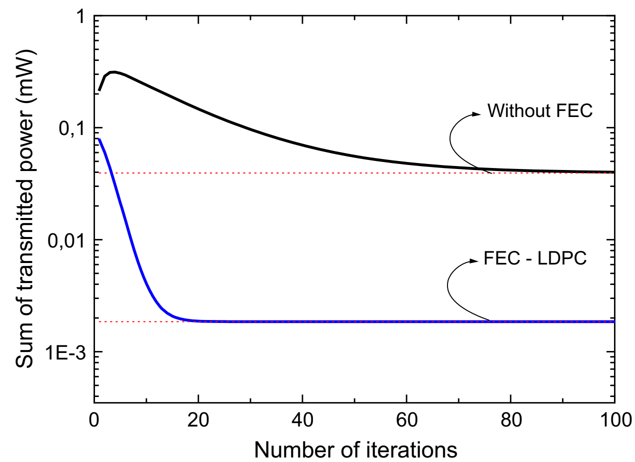

Fig. 7 Optimum transmitted sum of transmitted power for all network nodes

imum energy efficiency allowed for schemes with FEC and without FEC indicated by horizontal lines (dash lines) has been obtained via matrix inversion procedure, which presents high performance in terms of attainable energy efficiency but unacceptable computational complexity when compared with iterative DPCA procedures [25]. Hence, the matrix inversion procedure has been deployed as a reference just to validate/corroborate our numerical results.

It can be observed in Fig. 5 that the energy efficiency reaches the target value (horizontal line) when the iterations increase for each transmitted node, i.e., the nodes where each optical code was originated. The target of energy efficiency for all nodes is equal, and if the perfect power balancing was assumed, then it can be shown that the number of nodes limits the maximum energy efficiency [11]. As expected, the energy efficiency for OCDMA network with FEC is higher than the energy efficiency for OCDMA network without FEC, even when the power consumption and bandwidth occupancy are considered for the FEC implementation. Furthermore, the FEC capability to error correction increases the global energy efficiency of the OCDMA network. The variation of EE determinate by the relation $\Delta\text{EE} = (E_{\text{FEC}} - E_{\text{no-FEC}})\,/E_{\text{FEC}}$ is 15.61 % between the situations with and without FEC. In this context, it is worth to notice the capability of FEC to increase the energy efficiency of the OCDMA network considering different number of nodes.

The efficiency for OCDMA networks with different number of nodes is corroborated by Fig. 6 for OCDMA networks with 8, 16 and 32 nodes. Indeed, one can observe from Fig. 6 that the increasing nodes affect the energy efficiency for both the cases, with FEC and without FEC. Furthermore, the numerical results reveal that increasing the number of nodes from 8 to 16 and 32 results in a variation of the energy efficiency of $\Delta\text{EE} = 13.14$–14.21 and 15.61 %, respectively. This effect is directly related to the MAI rising which of course increases with the number of active nodes. An error occurs when cross-correlational pulses from the $(K - 1)$ interfering optical codes built up to a level higher than the autocorrelation peak, changing a bit zero to a bit one and vice versa. Furthermore, the FEC capability to correct errors when the MAI increases, associated with low power consumption, effectively contribute to increase the energy efficiency of the OCDMA network.

Figure 7 depicts the optimum transmitted sum of transmission power for all network nodes considering 32 nodes for the cases with FEC and without FEC. The optimum transmitted sum of power has been obtained by the sum of power of all network nodes for the DPCA evolution and taking into account the matrix inversion plotted with the horizontal dotted lines.

The results from Fig. 7 illustrate the convergence of the sum of transmitted power from DPCA approach to the values calculated by matrix inversion, represented by horizontal dash lines. The intensity of the transmitted optical signal of each node is directly adjusted from the laser source with respect to the target SNIR. Distinct power levels are obtained with adjustable transmitters, and it results in the possibility to save up the power consumption. The results have shown the impact of FEC in the decreasing the transmitted power. The difference of the transmitted power between the scheme with FEC–LDPC and without FEC is approximately 12 dB. This value is in agreement with the difference of transmitted power according to the BER levels adopted in this work. The results have shown that adoption of FEC results in a faster convergence. This fact occurs because the required SNIR for system with FEC is lower than for schemes without FEC; this fact impacts on the DPCA velocity of the convergence [25].

The difference of sum of transmitted powers for OCDMA networks with different number of nodes is illustrated in

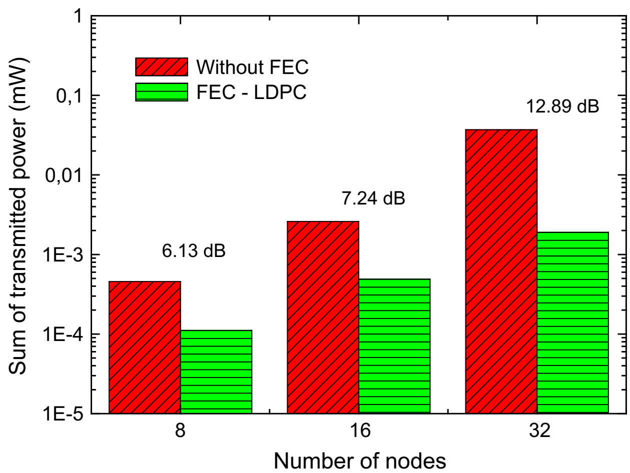

Fig. 8 Sum of transmitted nodes for OCDMA networks with different sizes for 8, 4 and 32 nodes, considering cases with FEC and without FEC

Fig. 8 for OCDMA networks with 8, 16 and 32 nodes. These numerical results show that the increasing the number of nodes affects the transmitted power and the difference of transmitted power between the cases with FEC and without FEC. Furthermore, the numerical results reveal that increasing the number of nodes from 8 to 16 and 32 results in an increasing difference of transmitted power of 6.13, 7.24 and 12.89 dB, respectively. Indeed, adopting FEC–LDPC implies a dramatic decrease in transmitted power. The capacity of LDPC error correction and their required lower SNIR requires a lower transmitted power; as a consequence, it will contribute to improve substantially the energy efficiency.

6 Conclusions

This work has analyzed the energy efficiency of optical code division multiple access (OCDMA) networks considering the transmitted power and forward error correction (FEC) low-density parity-check code (LDPC) type. The trade-off between FEC–LDPC and the optical layer energy efficiency considering the network capacity against the overall power consumption was investigated. The network power consumption model has considered the optical transmitter, receiver, optical amplifiers, FEC–LDPC parameters and the network infrastructure as encoders, decoders, star coupler and network control strategy. Furthermore, it has been derived an analytical expression relating the gain in the signal-to-noise-plus-interference ratio (SNIR) for FEC–LDPC scheme with the overall power consumption and bandwidth occupancy of the optical network. For the numerical results evaluated, a remarkable increase in the overall energy efficiency and a respective decrease in the transmitted power when FEC–LDPC is deployed has been observed.

Acknowledgments This work was supported in part by the Araucaria Foundation, PR, Brazil, under Grant 668/2014, National Council for Scientific and Technological Development (CNPq) of Brazil under Grant 304358/2012-6, 446995/2014-2 and State University of Londrina-Paraná State Government (UEL).

References

[1] Kilper, D., Bergman, K., Chen, V.W.S., Monga, I., Porter, G., Rauschenbach, K.: Optical networks come of age. In: OSA optics and photonics news, pp. 50–57 (2014)

[2] Yin, H., Richardson, D.J.: Optical Code Division Multiple Access Communication Networks: Theory and Applications. Springer-Verlag and Tsinghua University Press, Berlin (2009)

[3] Hinton, K., Baliga, J., Feng, M.Z., Ayre, R.W.A., Tucker, R.S.: Power consumption and energy efficiency in the internet. IEEE Netw. **25**(2), 6–12 (2011)

[4] Tucker, Rodney S.: Green optical communications—Part I: energy limitations in transport. IEEE J. Sel. Topics Quantum Electron. **17**(2), 245–260 (2011)

[5] Tucker, Rodney S.: Green optical communications—Part II: energy limitations in networks. IEEE J. Sel. Topics in Quantum Electron. **17**(2), 261–274 (2011)

[6] Wong, E.: Next-generation broadband access networks and technologies. J. Lightw. Technol. **30**(4), 597–608 (2012)

[7] Fouli, K., Maier, M.: Ocdma and optical coding: principles, applications, and challenges. IEEE Commun. Mag. **45**(8), 27–34 (2007)

[8] Durand, F.R., Galdino, L., Bonani, L.H., Barbosa, F.R., Abbade, M.L.F., Moschim, Edson: The effects of polarization mode dispersion on 2D wavelength-hopping time spreading code routed networks. Photon. Netw. Commun. **20**(1), 27–32 (2010). doi:10.1007/s11107-010-0242-6

[9] Durand, F.R., Abrão, T.: Distributed SNIR optimization based on the Verhulst model in optical code path routed networks with physical constraints. J. Opt. Commun. Netw. **3**(9), 683–691 (2011). doi:10.1364/JOCN.3.000683

[10] Mutafungwa, E.: Comparative analysis of the traffic performance of fiber-impairment limited WDM and hybrid OCDM/WDM networks. Photon. Netw. Commun. **13**, 53–66 (2007)

[11] Tarhuni, N., Korhonen, T., Elmusrati, M., Mutafungwa, E.: Power control of optical CDMA star networks. Opt. Commun. **259**, 655–664 (2006)

[12] Faucher, J., Ayotte, S., El-Sahn, Z., Mukadam, M.Y., Rusch, L.A., Plant, D.V.: A standalone receiver with MAI rejection, CDR and FEC for 2D λ-t OCDMA. IEEE Photon. Technol. Lett. **18**(20), 2123–2135 (2006)

[13] Ayotte, S., Rusch, L.A.: Increasing the capacity of SAC–OCDMA: forward error correction or coherent sources. IEEE J. Sel. Topics Quantum Electron. **13**(5), 1422–1428 (2007)

[14] Chang, F., Onohara, K., Mizuochi, T.: Forward error correction for 100 G transport networks. IEEE Commun. Mag. **48**(3), S48–S55 (2010)

[15] Huang, Yue-Kai, Baby, Varghese, Glesk, Ivan, Bres, Camille-Sophie, Greiner, Christoph M., Iazikov, Dmitri, Mossberg, Thomas W., Paul R. Prucnal, Fellow: Novel multicode-processing platform for wavelength-hopping time-spreading optical CDMA: a path to device miniaturization and enhanced network functionality. IEEE J. Sel. Top. Quantum Electron. **13**(5), 1471–1479 (2007)

[16] Sahuguede, S., Vergonjanne, A.J., Cances, J.P.: Performance of OCDMA system with FEC based on interference statistical distribution analysis. Eur. Trans. Telecomm. **21**(3), 276–287 (2010)

[17] Lundqvist, H., Karlsson, G.: On error-correction coding for CDMA PON. J. Lightw. Technol. **23**(8), 2342–2351 (2005)

[18] Liu, M., Hsu, Y., Jiang, J.: Utilization of LDPC code and optical hard-limiter in OCDMA communication systems. IEEE Photon. J. **6**(5), 1–11 (2014). doi:10.1109/JPHOT.2014.2331256
[19] Pillai, B.S., Sedighi, B., Guan, K., Anthapadmanabhan, N., Shieh, W., Hinton, K.J., Tucker, R.S.: End-to-end energy modeling and analysis of Long–Haul coherent transmission systems. J. Lightw. Technol. **32**(18), 3093–3111 (2014)
[20] Pereira, H., Chaves, D., Bastos-Filho, C., Martins-Filho, J.: OSNR model to consider physical layer impairments in transparent optical networks. Photon. Netw. Commun. **18**(2), 137–149 (2009)
[21] Aleksic, S.: Analysis of power consumption in future high-capacity network nodes. J. Opt. Commun. Netw. **1**(3), 245–258 (2009)
[22] Essiambre, R.-J., Kramer, G., Winzer, P.J., Foschini, G.J., Goebel, B.: Capacity limits of optical fiber networks. J. Lightw. Technol. **28**, 662–701 (2010)
[23] Barros, D., Kahn, J.: Comparison of orthogonal frequency-division multiplexing and on-off keying in amplified direct-detection single-mode fiber systems. J. Lightw. Technol. **28**(12), 1811–1820 (2010)
[24] Inaty, E., Shalaby, H., Fortie, P., Rusch, L.: Multirate "Optical fast frequency hopping CDMA system using power control". J. Lightw. Technol. **20**(2), 166–177 (2003)
[25] Durand, F.R., Filho, M.S., Abrão, T.: The effects of power control on the optical CDMA random access protocol. Opti. Switch. Netw. **9**(1), 52–60 (2012). doi:10.1016/j.osn.2011.06.002

Fábio Renand Durand received an M.S. degree in electrical engineering from the São Carlos Engineering School of São Paulo State, Brazil, in 2002 and a Ph.D. degree in electrical engineering from the State University of Campinas (UNICAMP), São Paulo, Brazil, in 2007. Now he is a Professor at Technologic Federal University of Parana (UTFPR) at Cornelio Procopio, PR, Brazil. His research interests are photonic technology, WDM/OCDM networks, heuristic and optimization aspects of OCDMA networks and PMD impairments.

Taufik Abrão (SM'12) received the B.S., M.Sc., and Ph.D. degrees in electrical engineering from the Polytechnic School of the University of São Paulo, São Paulo, Brazil, in 1992, 1996 and 2001, respectively. Since March 1997, he has been with the Communications Group, Department of Electrical Engineering, Londrina State University, Londrina, Brazil, where he is currently an Associate Professor of communications engineering. In 2012, he was an Academic Visitor with the Communications, Signal Processing and Control Research Group, University of Southampton, Southampton, UK. From 2007 to 2008, he was a Postdoctoral Researcher with the Department of Signal Theory and Communications, Polytechnic University of Catalonia (TSC/UPC), Barcelona, Spain. He has participated in several projects funded by government agencies and industrial companies. He is involved in editorial board activities of six journals in the communication area, and he has served as TPC member in several symposium and conferences. He has been served as an Editor for the IEEE COMMUNICATIONS SURVEYS & TUTORIALS since 2013. He is a member of SBrT and a senior member of IEEE. His current research interests include communications and signal processing, specially the multi-user detection and estimation, MC-CDMA and MIMO systems, cooperative communication and relaying, resource allocation, as well as heuristic and convex optimization aspects of 3G and 4G wireless systems. He has co-authored more than 170 research papers published in specialized/international journals and conferences.